

Contents lists available at ScienceDirect

#### Electrochimica Acta

journal homepage: www.elsevier.com/locate/electacta



### Optimization of electrochemical time of flight measurements for precise determinations of diffusion coefficients over a wide range in various media



Jonathan Moldenhauer <sup>a</sup>, Catherine Sella <sup>b</sup>, Becca Moffett <sup>a</sup>, Joel Baker <sup>a</sup>, Laurent Thouin <sup>b</sup>, Christian Amatore <sup>b, c</sup>, Stefan M. Kilyanek <sup>a</sup>, David W. Paul <sup>a, \*</sup>

- <sup>a</sup> Department of Chemistry and Biochemistry, University of Arkansas, 1 University of Arkansas, Fayetteville, AR, 72701, USA
- <sup>b</sup> PASTEUR, Département de Chimie, École Normale Supérieure, PSL University, Sorbonne Université, CNRS, 75005, Paris, France
- <sup>c</sup> State Key Laboratory of Physical Chemistry of Solid Surfaces, Department of Chemistry and Chemical Engineering, Xiamen University, Xiamen, 361005, China

#### ARTICLE INFO

# Article history: Received 4 March 2020 Accepted 20 March 2020 Available online 26 March 2020

Keywords: Electrochemical time-of-flight Diffusion coefficient Calibration curve Vanadium(III) acetylacetonate Generator-Collector mode

#### ABSTRACT

Diffusion coefficients are an important physical property to both physical and analytical electrochemistry and the role they play in sensors, batteries, and catalysis. In electrochemical time of flight (ETOF), the time needed for an electrochemically generated species to travel to an adjacent electrode is measured. Previously relegated to verifying diffusion modeling and theoretical work, ETOF is a powerful and elegant technique whose broad applicability has been overlooked. In the determination of diffusion coefficients, ETOF does not require setting delicate hydrodynamic conditions required by rotating ring disk (RDE) methods. In addition, no foreknowledge about the complete electrochemical mechanistic system, nor about its electron stoichiometry is required. ETOF is ideal for determining the diffusion coefficients for non-elucidated systems, such as for short-lived intermediates assuming they survive ETOF travel time. Here we report the construction of a universal empirical calibration curve for the determination of diffusion coefficients using experimental parameters optimized by computer modeling. Using a platinum micro electrode array, diffusion coefficients were determined for a variety of species including ferrocenium, ruthenium (III) bisbipyridine dichloride, and vanadium (III) acetylacetonate, some of which being previously unreported. The elegance of the method is that the calibration curve constructed with a few well-established species in a given electrolyte can be used for any species in any electrolyte.

Published by Elsevier Ltd.

#### 1. Introduction

In addition to being a fundamental property of any solute, diffusion coefficient values are crucial in several applications of electrochemistry. Diffusion plays a pivotal role in analytical or mechanistic investigations as well as for amperometric and potentiometric sensors [1], electrosynthesis [2], redox flow batteries [3], etc. These are all applications where the electrical response depends on the diffusion of molecules to and from an electrode. Typically, precise diffusion coefficients values, D, are determined either by electrochemical means using for example scanning electrochemical microscopy (SECM) [4–9] or rotating ring disk (RDE)

methods [10–17]. RDE methods are based on the Levich equation, Eq. (1). The RDE limiting diffusion current plateau value,  $i_{\text{Lev}}$ , is directly proportional to the two-thirds root of diffusion coefficient of the analyte, D. However, prior knowledge of the number of electrons transferred, n, the active area of the electrode, A, the kinematic viscosity of the supporting electrolyte,  $\nu$ , and the analyte concentration of the bulk solution,  $C_{\text{S}}$  [12] is also required. To determine the diffusion coefficients  $i_{\text{Lev}}$  values are plotted as a function of  $\sqrt{\omega}$ . The slope is determined and D is calculated.

$$i_{\text{Lev}} = 0.620nFAD^{\frac{2}{3}}\omega^{\frac{1}{2}}v^{\frac{-1}{6}}C_{\text{S}}$$
 (1)

This can lead to experimental challenges, as several of the terms in the slope of Eq. (1) must be known to calculate the diffusion coefficients. Due to specific mechanistic circumstances, n may not be an exact integer [18] since it may vary continuously with the

<sup>\*</sup> Corresponding author. E-mail address: dpaul@uark.edu (D.W. Paul).

timescale of the experiment [19]. Kinematic viscosity of the solution and the concentration of the analyte can be determined through additional experiments, but this makes for an additional burden. In addition, every electroactive analyte experiences different diffusion coefficient values in different media. Using RDE to determine diffusion coefficients requires a new Levich plot to be constructed for each Red/Ox analyte every time any of the terms n, A,  $\nu$ , and  $C_S$  change. Finally, it should be noted that Eq. (1) relates to the diffusion coefficient of the bulk electroactive species in solution and not the product(s) formed by reduction or oxidation. Diffusion coefficients of reaction products can be measured by RRDE, but that technique is not used routinely for this purpose.

It is also possible to determine values of n and D simultaneously by comparing responses from a transient technique to that of a steady state technique at a microelectrode. However, in order to avoid biases introduced by the exact electrode surface area and size, the method requires the use of an internal standard with known n and D. The techniques also requires high experimental precision and accuracy. In addition, when n values are suceptible to a timescale due to kinetics, special care is required to compare responses corresponding to the same time-scale as detailed in the reference [18].

In SECM, the probe serves as the detecting electrode for a redox species generated at the surface under examination. The diffusion coefficient is determined by measuring the time of maximum collection at different probe distances from the surface. In this respect, SECM and electrochemical time of flight (ETOF) [20] are formally identical as both involve generation and collection of the species of interest. SECM and ETOF approaches differ only in that SECM relies on collector-generator current feedback magnitude (viz., on collection efficiencies), while ETOF relies on direct measurements of travel times of the generated species of interest between its source (the generator electrode) and its sink (the collector electrode(s) [21]. Additionally, SECM-based methods may not be applicable in structured electrolyte media such as polymers or solgel materials in which diffusion coefficient values may be required [17].

#### 1.1. ETOF principle

ETOF is a well established method, first developed by Royce Murray [22] to measure diffusion coefficients. In this work we wish to introduce a new and universal application of this principle to measure diffusion coefficients in any medium and electrolyte based on reference measurments made in a separate electrolyte. For this reason let us first recall the principle and theoretical basis of ETOF to allow the introduction of this present application.

ETOF consists of measuring the time that a generated species takes to travel from one electrode to an adjacent detecting electrode; the travel time can then be related to the diffusion coefficient. Murray was interested in determining the apparent diffusion coefficients of electron-hopping across conducting polymers sandwiched between two electrodes. For ETOF travel time of maximum collection,  $t_{mc}$ , relates the diffusion coefficient, D, through Einstein's equation, (Eq. (2)), to the distance traveled or gap, g, between the two electrodes and a numerical dimensionless constant, K, that depends exclusively on the electrode array geometry. The latter does not depend on the electrochemical medium, nor on the half-life time,  $t_{1/2}$ , of the species of interest provided that  $t_{1/2}$  is greater than  $t_{mc}$ .

$$g = K\sqrt{Dt_{mc}} \tag{2}$$

K can be predicted computationally for generator-collector

systems having ideal geometries [23,24] or evaluated empirically based on calibrations performed for micro-systems of any geometry [25–27]. In the most popular procedure of ETOF, the generator is pulsed to a potential that generates a swarm of diffusible species, while the detector is held at a constant potential in order to rereduce or re-oxidize the generated species (Fig. 1A). These experiments have been limited to model compounds such as ruthenium ferricyanide hexamine 24, 26], [23,24], ymethylferrocenium [28] or the analyte of interest in a previous study [25]. Most of the literature reports the use of ETOF as a way to verify computational models of diffusion between electrodes, viz., as a way to assess experimentally the "ideality" of the microfabricated electrode pattern. The current ETOF approach has been to measure  $t_{mc}$  at various distances between the generating and detecting electrodes to determine diffusion coefficients, and then compare to the theoretical estimate. Here we point out that the practical applications of ETOF have been largely over looked, and ETOF is a simple technique capable of measuring the diffusion coefficients of a variety of substances in various media.

#### 1.2. Previous Work and Outline of this Work

Previously, some of us presented a novel data treatment for ETOF that provided a simple and elegant method for determining diffusion coefficients [29]. In this approach, a calibration curve is constructed by measuring the time of maximum collection ( $t_{\rm mc}$ ) between two parallel band electrodes in a microelectrode array having a single and constant distance, g, between the generator and collector electrodes. Using species with known diffusion coefficients as "standards" in the medium of interest,  $t_{\rm mc}$  is recorded for each electrochemically generated species. Rewriting Eq. (2) as

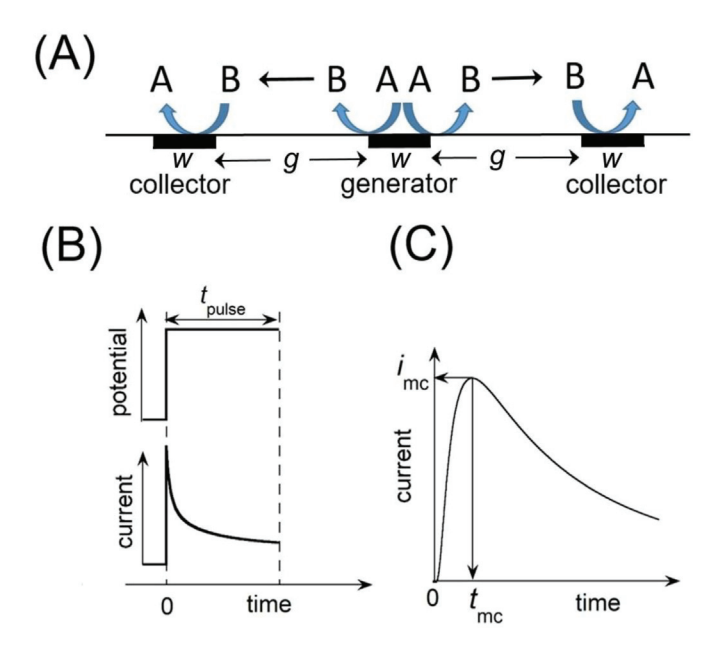


**Fig. 1.** The ETOF experiment. (A) Schematic cross section of the device considered in the ETOF experiments. g is the gap distance between the electrodes selected to operate as generator and collector electrodes. These electrodes are indicated by black rectangles embedded in the insulating plane. (B) Schematic time dependence of the potential pulse applied at the generator and of the resulting generator current. (C) Corresponding collector response characterized by a peak-shaped current with its maximum characterized by its current, time coordinates (imc, tmc). Note that the time scales in (B) and (C) are not identical, that in (C) being compressed vs that in (B).

$$\sqrt{t_{mc}} = \frac{g}{K\sqrt{D}} \tag{3}$$

and plotting  $\sqrt{t_{mc}}$  variations as a function of  $\frac{1}{\sqrt{D}}$  produces a calibration curve that is used to determine diffusion coefficients of unknown species regardless of other characteristics of the medium and of the species.

In this paper, we have expanded electrolyte solutions to include non-aqueous solvents. In addition, computer modeling assisted the optimization of the pulse widths for the generator so that diffusion coefficients could be determined over a large dynamic range with an adequate precision and accuracy.

## 2. Theoretical optimization of precision and accuracy in ETOF measurements

As shown in Fig. 1, applying a sufficiently brief potential pulse to the generator electrode generates a local concentration of B in its immediate vicinity [30]. Diffusional broadening of this concentration pulse over the insulating gap g allows capture by the collector(s); because of the short duration of the generator pulse, B is rapidly exhausted. Hence, a peak-shaped current response is expected at the collector [23,31] whose maximum time position,  $t_{mc}$ , in a static solution is directly correlated to the time-of-flight (TOF) of species B. However, if the pulse width  $(t_{pulse})$  is too long, and the electrochemical detection of B regenerates A at the collector electrode, the regenerated species A may then diffuse back to the generator electrode where it can again form B. This redox-cycling leads to an inaccurate value for D. Specifically, the result of redoxcycling is that the time position of the maximum collector current  $t_{mc}$  shifts towards greater values since it now represents a convolution between the shortest TOF and the maximum redoxcycling efficiency. In the absence of any noise or background interference, a  $t_{pulse}$  value preventing redox-cycling gives the most accurate values for D of species B. At the other extreme, too short t<sub>pulse</sub> values lead to generating small quantities of B which are difficult to detect with proper precision at the collector, lowering the accuracy of  $t_{mc}$  determination. This experimental conflict between accuracy and precision indicates that the  $t_{
m pulse}$  value should be maximized, yet less than  $t_{\text{pulse}}^{\text{max}}$ , the value beyond which redoxcycling contributions will alter the accuracy. Modeling the diffusion demonstrates that the  $t_{
m pulse}^{
m max}$  value is not universal but depends on the rate of diffusion of the species of interest over the insulating gaps. However, even an unknown diffusion coefficient can be approximated by simple measurements of  $t_{mc}$ .

The present work shows that modeling can guide the selection of experimental parameters for ETOF resulting in the accurate determination diffusion coefficients, as well as further validating the experimental principle of determining diffusion coefficients by ETOF. Because K and g are geometric parameters, independent of the properties of the electrolyte medium and of the substrate whose D value is sought to be measured, it is possible to construct an empirical calibration curve relating D and  $t_{mc}$  values (Eq. (3)) using a series of parallel microelectrode arrays. Once the calibration curve is constructed in one medium, the same microelectrode array (with the same geometry) may then be used to determine diffusion coefficients of other species in any media. One can measure the  $t_{\rm mc}$ value of an electrogenerated species in any medium, and take that  $t_{\rm mc}$  to the calibration curve and estimate the D for that species in the electrolyte medium used. There is one caveat. Since the diffusion coefficient for a species may vary greatly from one medium to the next,  $t_{\text{pulse}}^{\text{max}}$  along with  $t_{mc}$  may vary, leading to an inaccuracy in the determination of diffusion coefficient caused by redox-cycling

(vida supra). For these reasons, we wish to present the results of a simplified theoretical analysis aimed to evaluate the relationship between  $t_{\rm pulse}^{\rm max}$  and  $t_{\rm mc}$  values.

#### 2.1. Numerical Simulations using COMSOL

Our theoretical analysis was performed using COMSOL simulations of ideal micro-device systems consisting of three parallel microband electrodes of common width, w, separated by insulating gaps of common width g with the array being imbedded flat in an insulating plane (Fig. 1A) [20,29]. Owing to its scope, this theoretical analysis was simplified assuming that the electrodes present no vertical edges and that no metallic conductor was located within the gap separating the generator and collector electrodes in order to avoid complications related to any bipolar activity that may be induced over such isolated conductors [32, 33].

We assume that the semi-infinite bulk electrolyte contains only species A. Species A reduces or oxidizes at the generator electrode whose potential is stepped for a fixed time duration,  $t_{\rm pulse}$ , and then returned to an open circuit potential (Fig. 1B). This generates a peak-shaped current response (Fig. 1C) characterized by its current maximum,  $i_{\rm mc}$ , and its time position,  $t_{\rm mc}$ , after the beginning of the pulse (t=0).

Fig. 2A illustrates the outcome of the corresponding simulations showing how the collector peak-shaped response varies when  $t_{\text{pulse}}$ increases. Fig. 2B reports the variations of  $t_{\rm mc}$  normalized to its ideal limit when  $t_{\text{pulse}} \rightarrow 0$ , as a function of  $t_{\text{pulse}}$  also normalized to the same limit. The dimensionless presentation of the theoretical results in Fig. 2B is independent of the exact nature of the redox system considered and of the geometry of device used, provided that the width, w, of the band electrodes remains sufficiently small vs the gap, g. The results in Fig. 2B are evidence that t<sub>pulse</sub>/t<sub>mc</sub> must be smaller than 0.03-0.04 to yield accurate measurements. This constraint is independent from the exact mechanisms involved in the electrochemical processes investigated provided that the species B generated at the generator by reduction or oxidation of species A is the only one that is collected at the collector. In the case here, the generator and collector potentials are experimentally chosen so that the reduction of A (or its oxidation) and the detection of B are performed at the current limiting plateaus of the corresponding electrochemical waves. B could be a follow-up product resulting from an EC mechanism at the generating electrode, e.g.:  $A \pm e^- \rightarrow A^{\pm} \rightarrow B$ . One constraint in such case is that the half-life time,  $t_{1/2}$  of A<sup>±</sup>, the primary intermediate formed by the reduction of A, must be negligible compared to  $t_{mc}$ . If that were not the case, the ETOF method would provide a "mixed" diffusion coefficient convoluting those of B and A±. Therefore, the ETOF method should be reserved for the analysis of redox systems whose CV simultaneously displays the voltammetric waves of A (forward scan) and B (backward scan) containing no intermediate wave within a single voltammetric scan. The time scale is such that the scan rate,  $v_{mc}$ , should be approximately  $v_{mc} \sim RT/(Ft_{mc})$  where R is the gas constant, F is the Faraday value, and T is the absolute temperature [34]. As discussed later we discovered such a case when determining the diffusion coefficient for the oxidation product of VO(acac)<sub>2.</sub> (vida infra) whose oxidation has been reported to provide a chemical conversion to V (acac)<sub>3</sub> [35].

#### 2.2. Conclusions from Simulations with COMSOL

The first conclusion of this theoretical analysis is that the duration of the generator pulse duration,  $t_{\text{pulse}}$ , should not exceed a maximum value being ca. 0.03 to 0.04 times that of the minimal value of the experimentally determined  $t_{\text{mc}}$ . This is especially

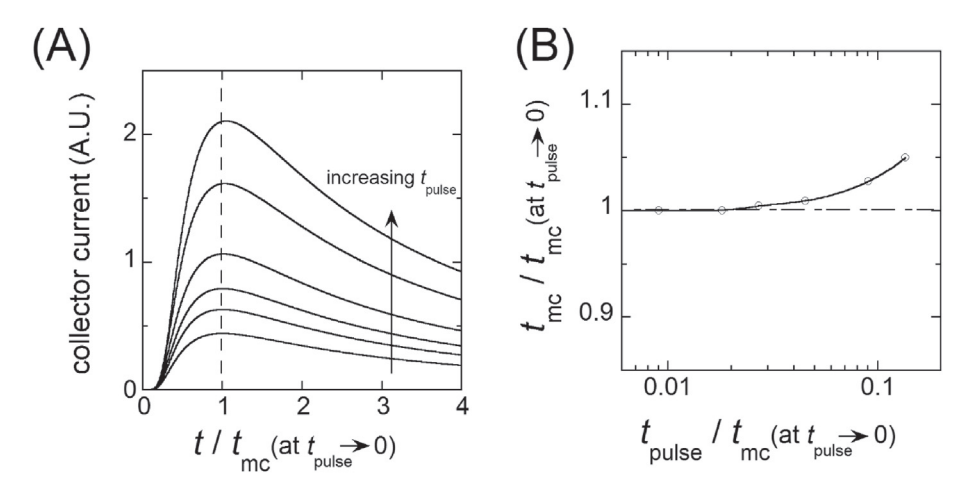


Fig. 2. The influence of  $t_{\text{pulse}}$  on the relative intensity and time position of the collector peak. (A) Collector current responses for increasing tpulse values as determined numerically for the system in Fig. 1A. tmc tends towards a constant value, independent of tpulse when tpulse  $\rightarrow$  0. (B) Variation of the ratio tmc /(tmc at tpulse  $\rightarrow$  0) as a function of tpulse /(tmc at tpulse  $\rightarrow$  0); note that the abscissa in B is in log scale.

important when dealing with an unknown system.  $t_{\rm mc}$  can be evaluated from several experiments at different  $t_{pulse}$  to respect the criterion in Fig. 2B. A second conclusion is that the ETOF can determine the diffusion coefficient of any species that is the product of the reduction or oxidation of a precursor species, A or a chemical product from an EC mechanism provided the  $t_{1/2}$  of its formation from the primary generated product is then negligible vs  $t_{\rm mc}$ .

#### 3. Experimental

#### 3.1. Materials and electrochemical device

All electrochemical measurements were performed using a CHInstruments 750a bipotentiostat. The time duration and application of  $t_{\rm pulse}$  for the generator was controlled by National Instruments LabVIEW software. Microband electrode arrays of 16 platinum or gold fingers, 2 mm long, 25  $\mu$ m wide with gaps of 25  $\mu$ m were fabricated at the Arkansas High Density Electronics Center (HiDEC). Using either one of these arrays provided essentially identical results. A saturated KCl Ag/AgCl reference electrode was used in aqueous solutions. A saturated calomel electrode fitted with an organic solvent bridge made with TBAPF<sub>6</sub> in the solvent considered was constructed for use in organic solvents. Measurements were performed in a VAC-atmospheres glovebox with a purified anhydrous nitrogen atmosphere. The atmosphere was purged extensively between experiments while the SCE was sealed in a gastight container.

#### 3.2. Chemicals

Diffusional reference "standards", potassium ferrocyanide (Certified ACS grade, Fischer), potassium ferricyanide (Certified ACS grade, Fischer), ruthenium (III) hexamine chloride (Alfa Aesar), ferrocene (98% Sigma Aldrich), ferrocene acetic acid (98% Sigma Aldrich), and ruthenium bisbipyridine dichloride (Ru (bpy)<sub>2</sub>Cl<sub>2</sub>) (97% Sigma Aldrich) were used as received. Two electrolyte solutions were made: one (aqueous) consisting of 0.1 M KCl (ACS grade, J.T. Baker); the other (organic) consisting of 0.1 M TBAPF<sub>6</sub> (98%, Sigma Aldrich) in acetonitrile (HPLC Grade, Fischer). The vanadyl acetylacetonate (VO(acac)<sub>2</sub>) was synthesized from Vanadium(V) Oxide (98%, Sigma Aldrich) and acetylacetone (Reagent Plus grade,

Sigma Aldrich) according to the literature method and was recrystallized from dichloromethane [36].

#### 3.3. Conditions of electrochemical measurements

5 mM solutions were made of each "reference" electroactive compound, i.e. those with known diffusion coefficients. Three equally spaced (gap distance of  $g=75~\mu m$ ) microband electrodes ( $w=25~\mu m$ ) were selected by pairing sets of microbands available in the microfabricated arrays to perform ETOF measurements. The other 13 microbands present in the array were left open-circuit. The generator electrode potential was imposed for a time duration,  $t_{\rm pulse}$ , and then open circuited to minimize current feedback. The potentials on the two flanking collector electrodes remained continuously poised [29].

The applied potentials values were determined using cyclic voltammetry (CV). CV was also used to ensure that the condition  $t_{1/2}$  $_2$  «  $t_{
m mc}$  was valid for complex mechanisms. Measurements were performed in either 0.1 M KCl or in 0.1 M TBAPF<sub>6</sub>/acetonitrile. For the latter case, unless otherwise noted, all potentials were referenced to a SCE using a double salt bridge. The potential window for the CV for ferrocene and ferrocenyl acetic acid solutions was from  $-0.6\ V$  to  $+0.8\ V$ , and the ETOF potentials were selected as follows. For experiments with ferrocene, the generator was pulsed to +0.8 V while the collectors were held at +0.1 V. For ferrocene acetic acid, the generator was pulsed to +0.5 V while the collectors were held at +0.1 V. The CV potential window for Ru(II) (bpy)<sub>2</sub>Cl<sub>2</sub> was +0.5 V to -0.2 V and the ETOF potentials were set at +0.5 V for the generator pulse and -0.1 V for the collectors. The ferrocene/ ferrocenium have known diffusion coefficient from the literature [37] and Ru(II) (bpy)<sub>2</sub>Cl<sub>2</sub> was compared to an estimated diffusion based on its mass [38].

The mechanism occurring during the  $V^{IV}O(acac)_2$  oxidation wave is complex [35], possibly leading to formation of  $V(acac)_3$  (see Appendix A). The potential window for the CV of  $VO(acac)_2$  was thus extended from +2.0 V to -2.0 V to identify the ETOF potentials. These were set at +1.0 V for the generator pulse and -1.5 V for the collectors in order to determine the diffusion coefficient of  $V(acac)_3$ , the suspected product. Under these conditions, only two waves were observed, the oxidation one of  $V^{IV}O(acac)_2$  and the reduction one of its oxidation product observed during the backward scan [35].

#### 4. Results and discussion

#### 4.1. ETOF calibration curve

An experimental ETOF calibration curve (Fig. 3) was constructed with a constant value of  $t_{\rm pulse}=61$  ms using the same electrode array as before [29]. A calibration curve was constructed based on the experimental  $\sqrt{t_{mc}}$  values determined in 0.1 M KCl, using three "reference" species, formed at the generator. The respective D values taken from literature reports, vis. ferrocyanide ( $D=6.5\times10^{-6}~{\rm cm^2/s}$ ) [24], ferricyanide ( $D=7.2\times10^{-6}~{\rm cm^2/s}$ ) [39], and ruthenium (II) hexamine ( $D=7.8\times10^{-6}~{\rm cm^2/s}$ ) [24]. The K constant in Eq. (3), was determined from the slope (3.23 ( $\pm0.03$ ) x10<sup>-3</sup>) of the regression line after forcing the line through the origin in order to comply with the theory. A band separation of  $g=75~{\rm \mu m}$  provided a value for  $K=2.32~(\pm0.02)$ . The  $t_{mc}$  measured for these three "reference" species using a  $t_{\rm pulse}=61~{\rm ms}$ , satisfied the criterion ( $t_{\rm pulse}/t_{\rm mc}=0.037$ ), developed by the modeling ensuring no recycling and sufficient collection current to determine  $t_{\rm mc}$  with precision.

Using this calibration curve, the diffusion coefficients values for the other species ferrocenium and ferrocenium acetic acid could be determined based on their  $t_{mc}$  values. However, the case of ferrocene/ferrocenium serves to illustrate the danger of using too large a value for  $t_{\text{pulse}}$ . The ferrocenium generated has a three times larger diffusion coefficient,  $D = 2.24 (\pm 0.07) \times 10^{-5} \text{ cm}^2/\text{s}$  [37], than those used to construct the calibration line in Fig. 3. Use of the same pulse width  $t_{\text{pulse}} = 61$  ms, resulted in a  $t_{\text{mc}}$  value of 0.93 s, which the calibration curve translated as a diffusion coefficient for ferrocenium of 1.22 ( $\pm 0.03$ )x10<sup>-5</sup> cm<sup>2</sup>/s, i.e., half the value of 2.24 ( $\pm 0.07$ )  $x10^{-5}$  cm<sup>2</sup>/s reported in the literature [37]. Ferrocenium diffuses rapidly making  $t_{\text{pulse}}/t_{\text{mc}} = 0.065$ , resulting in recycling, and yielding an incorrect value. We described this result to illustrate the necessity of respecting the criterion in Fig. 2B, i.e.,  $t_{pulse}/t_{mc} < 0.037$ .  $t_{\text{pulse}}$  was then decreased from 61 ms to 24 ms, and the resulting diffusion coefficient value of 2.4 ( $\pm 0.1$ )x10<sup>-5</sup> cm<sup>2</sup>/s for ferrocenium, falling within 7% of the reported literature value in acetonitrile. Fig. 3 shows the relative positions of the two corresponding data points for ferrocenium using both values for  $t_{\rm pulse}$ . A similar yet inaccurate value was obtained for the diffusion coefficient of ferrocenium acetic acid (not shown). Using  $t_{\rm pulse}=61$  ms afforded  $D=1.10~(\pm0.05)~{\rm x}10^{-5}~{\rm cm}^2/{\rm s}$  for ferrocenium acetic acid using the calibration line in Fig. 3, or half the value of the predicted based on its molecular weight (38). In the case of determining the diffusion coefficient for an unknown species, this illustrates the importance of verifying that the  $t_{\rm pulse}/t_{\rm mc}$  criterion be satisfied; this is easily determined as  $t_{\rm pulse}$  is selected and  $t_{\rm mc}$  is measured.

## 4.2. Aqueous diffusion coefficient calibration curves can extend to organic solvents

The previous calibration curve in Fig. 3 was constructed using literature values for diffusion coefficients (Ds) and measuring  $t_{mc}$  in 0.1 M KCl for each "reference" species. However, the value of the constant K is an intrinsic characteristic of the microelectrode array and not of the redox system investigated nor the electrolyte medium used. Hence, the calibration curve in Fig. 3 should be valid in all electrolytes even if the curve was constructed using different redox couples in 0.1 M KCl. To test the validity of this prediction,  $t_{\rm mc}$ was determined in 0.1 M TBAPF<sub>6</sub>/acetonitrile for the oxidation products of ferrocene and Ru (bpy)<sub>2</sub>Cl<sub>2</sub>. The corresponding results are shown in Fig. 4, the dotted regression line being taken from Fig. 3, using 0.1 M KCl electrolyte. Using the  $t_{\rm mc}$  values taken in acetonitrile, and the calibration curve constructed using 0.1 M KCl electrolyte, the resulting diffusion coefficients for ferrocenium [37] and Ru (bpy)<sub>2</sub>Cl<sub>2</sub><sup>+</sup> [38] matched perfectly the literature data for their diffusion coefficients in acetonitrile. This validates our claim that diffusion coefficient calibration curves constructed using a few "reference" species in a given electrolyte can then be used to determine diffusion coefficients in other electrolytes including organic media. As we will note in the next section the ETOF method is not at all restricted to A/B redox systems involving a single

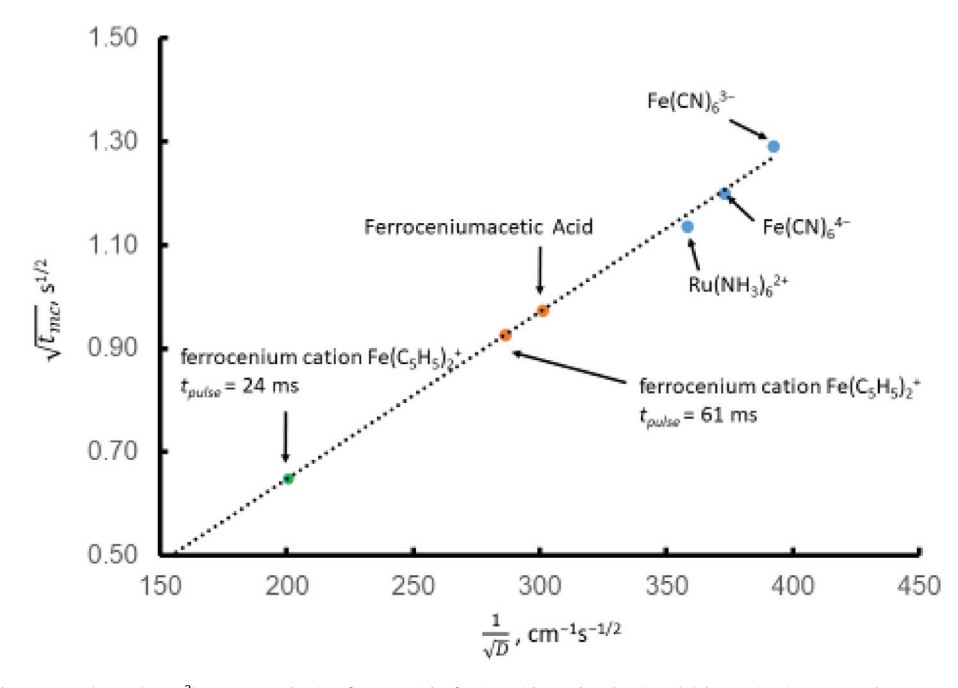
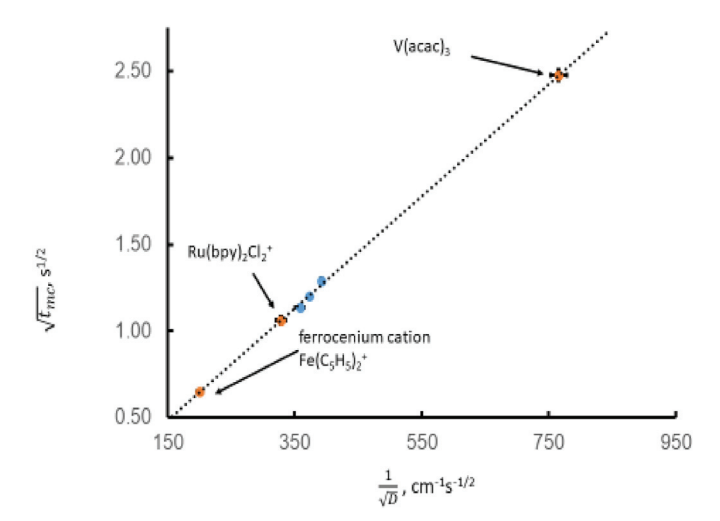


Fig. 3. Calibration curve (slope  $= 3.23(\pm 0.03) \times 10^{-3}$ ) constructed using ferrocyanide, ferricyanide, and ruthenium (II) hexamine in 0.1 M KCl aqueous solution based on tmc values determined from ETOF experiments using tpulse = 61 ms and known diffusion coefficients of the generated species (indicated on the graph). The dotted line represents the equation  $= 3.23(\pm 0.03) \times 10^{-3}$ . The incorrect tmc values determined for ferrocenium and ferrocenium acetic acid in acetonitrile using tpulse = 61 ms are shown by orange circles while the correct one measured for ferrocenium using tpulse = 24 ms is shown by a green point.



**Fig. 4.** Use of the calibration curve, reported in Fig. 3 to determine diffusion coefficients in acetonitrile from tmc values determined in acetonitrile with 0.1 M TBAPF<sub>6</sub> as the supporting electrolyte for generated species: Ferrocenium, Ru(bpy<sub>2</sub>)Cl $\frac{1}{2}$ , and V(acac)<sub>3</sub>. In order to fulfill the criterion  $t_{pulse} / t_{mc} < 0.037$ ,  $t_{pulse} = 24$  ms was used for Ferrocenium while  $t_{pulse} = 61$  ms was used for the three other species. Blue circles represent the set of data determined for generated species Ru(NH<sub>3</sub>) $_6^2$ +, Fe(CN) $_6^3$ - and Fe(CN) $_6^4$ - in 0.1 M KCl aqueous solution, while orange circles represent the set of data determined in acetonitrile / 0.1 M TBAPF<sub>6</sub>.

reversible electron transfer step but is also applicable to more complex kinetic sequences, as in the case reported for VO(acac)<sub>2</sub> [35].

#### 4.3. ETOF applied to VO(acac)<sub>2</sub> in acetonitrile/0.1 M TBAPF<sub>6</sub>

As mentioned in the Experimental section, the electrochemical oxidation of vanadyl acetylacetonate, VO(acac)2 is reported to lead to V(acac)<sub>3</sub> [35]. The generation of V(acac)<sub>3</sub> from VO(acac)<sub>2</sub> has been previously studied [35,40-42], but a definitive mechanism of reaction following VO(acac)<sub>2</sub> oxidation could not be presented. However, the following critical observations were made. 1) The CV reduction wave of the oxidation product of VO(acac)<sub>2</sub> and that of  $V(acac)_3$  appear to be the same CV. 2) CV reduction of  $V(acac)_3$ affords the oxidation wave of VO(acac)<sub>2</sub> and 3) the oxidation products of V(acac)<sub>3</sub> formed by controlled potential coulometry can re-form VO(acac)<sub>2</sub>. With these critical observations in hand it is reasonable to conclude that oxidation of VO(acac)2 forms an intermediate that upon some combination of chemical steps and electron transfer from a variety of homogeneous vanadium species likely leads to the formation of V(acac)<sub>3</sub> through a complex but pseudo-reversible redox system.

The ETOF method amounts to determining the diffusion coefficient of the species generated at the generator and not of that present in the solution bulk. The VO(acac)<sub>2</sub>/V(acac)<sub>3</sub> system offered a good opportunity to test the applicability of ETOF when the electron stoichiometry of the electrochemical reaction(s) producing the species of interest (here V(acac)<sub>3</sub>) is complex and a priori unknown under analytical conditions. Ultimately ETOF determined the diffusion coefficient for the products of reaction to be consistent with previously measured diffusion coefficients for V(acac)<sub>3</sub> [3] offering support to the mechanistic proposals of previous studies suggesting the generation of V(acac)<sub>3</sub> from VO(acac)<sub>2</sub> and vice versa. However, depending on the side products co-generated with V(acac)<sub>3</sub>, the electron stoichiometry is impossible to ascertain due to the expected involvement of father-son reactions (see Appendix A)

The diffusion coefficient of V(acac)<sub>3</sub> in acetonitrile with 0.1 M

TBAPF<sub>6</sub> as the supporting electrolyte was thus deduced experimentally based on the corresponding  $t_{\rm mc}$  value using the calibration curve without any hypothesis about its exact nature. This afforded a value of 1.71 ( $\pm 0.08$ )x10<sup>-6</sup> cm²/s (Fig. 4). Such value is in total disagreement with the estimated diffusion coefficient based on the molecular weight of its primary oxidation intermediate V<sup>V</sup>O(acac)½. Conversely, a diffusion coefficient has been reported for V<sup>III</sup>(acac)<sub>3</sub> [3], viz., 1.8 × 10<sup>-6</sup> cm²/s, being only 5% greater than the value measured by ETOF. This finding demonstrates the utility and elegance of the ETOF method allowing for the determination of a diffusion coefficient without a complete mechanistic understanding of the reaction occurring and allowing for identification of the products offering further support for a mechanistic proposal.

#### 5. Conclusions

This work shows that ETOF approach described here is an elegant, effective, and simple method that easily determines the diffusion coefficient of the product of a redox reaction in any medium and even when the product is formed through a complex and possibly unknown mechanistic sequence. The ETOF approach relies only on the duration of the diffusional transport between a generator electrode where the species of interest is formed and a collector(s) electrode(s) at which it can be detected electrochemically. In contrast to other methods, ETOF does not rely on the electrochemical current intensities measured. This unique advantage of the ETOF approach has been successfully illustrated in the context of vanadyl acetylacetonate, VO(acac)<sub>2</sub>, oxidation that underwent a complex mechanism with unknown fractional electron stoichiometry.

A second unique advantage of the ETOF method is that the relationship between the measured time of flights,  $t_{\rm mc}$ , and the sought diffusion coefficients, D, are independent of the electrolyte/solvent media in which the ETOF measurements are performed. Instead, ETOF measurements depend exclusively on the geometrical characteristics of the microband electrode array used. The lack of dependence on solvent/electrolyte media has been illustrated by establishing a calibration curve,  $\sqrt{t_{mc}} \propto 1/\sqrt{D}$  (Fig. 3), based on the measurements of  $t_{\rm mc}$  values in 0.1 M KCl for a series of species whose diffusion coefficients were reported in the literature and validating its use in 0.1 M TBAPF<sub>6</sub>/acetonitrile (Fig. 4).

Albeit these are important and unique advantages, it is emphasized that a proper use of the ETOF method requires that the duration,  $t_{\rm pulse}$ , of the potential pulse applied to the generator electrode is sufficiently small compared to the experimental time of flight,  $t_{\rm mc}$ . This must be ensured experimentally as shown in Fig. 2B, since for a given species using too large  $t_{\rm pulse}/t_{\rm mc}$  values produces an increasing drift of  $t_{\rm mc}$  values. Numerical modeling with COMSOL, was especially useful in establishing quantitatively the criterion fixing the upper limit of  $t_{\rm pulse}$  values for a given experimental value of the time-of-flight  $t_{\rm mc}$ 

#### **Declaration of competing interest**

The authors declare that they have no known competing financial interests or personal relationships that could have appeared to influence the work reported in this paper.

#### Acknowledgements

In Fayetteville, this work was supported by the Arkansas Applied Biosciences Institute and the National Science Foundation (CHE-1263119/REU). SMK acknowledges funding from the National Science Foundation (CHE-1654553). In Paris, this work was supported

by in parts by Ecole Normale Supérieure, PSL Research University, CNRS (UMR8640), and Sorbonne University. J.M. specially thanks Professor Ingrid Fritsch for helpful discussions and also Nandita Halder & Errol Porter for the fabrication of microelectrode arrays. C.A. thanks the University of Xiamen, China, for his Distinguished Scientist position.

#### Appendix A

The electron stoichiometry of V<sup>IV</sup>O(acac)<sub>2</sub> oxidation at the generator electrode is expected to generate the cation  $V^{V}O(acac)^{\frac{1}{2}}$ as the primary intermediate. The oxidation numbers of the vanadium center are noted in the following to help in recognizing father-son sequences:

 $V^{IV}O(acac)_2 \leftrightarrow V^{V}O(acac)_2^+ + e^-$  (expected but not seen) (A.1).

The chemical instability of this primary intermediate was confirmed by the absence of a reduction wave for  $V^VO(acac)_2^+$  in the CV (Eq. A1). Owing to the reported instability of V<sup>IV</sup>O(acac)<sub>2</sub> in the presence of its oxidation product  $V^{IV}O(acac)_2^+$  [35],  $V^VO(acac)_2^+$  is expected to undergo a rapid father-son follow-up mechanism [19] in the presence of adventitious water:

 $V^{IVO}(acac)_2 + H_2O \leftrightarrow V^{IV}O(OH)(acac)_1 + Hacac (A.2)_1$ 

 $V^{V}O(acac)_{2}^{+} + Hacac \leftrightarrow V^{V}(acac)_{3}^{2+} + OH^{-} (A.3).$   $V^{V}(acac)_{3}^{2+} + 2 V^{IV}O(acac)_{2} \rightarrow 2 V^{V}O(acac)_{2}^{+} + V^{III}(acac)_{3} (A.4).$ 

Eqs. A1-A4 provide one possible mechanism for the extremely fast formation the neutral V<sup>III</sup>(acac)<sub>3</sub> species whose diffusion over the generator-collector(s) gap would then be measured instead of that of the primary oxidation intermediate V<sup>v</sup>O(acac)<sub>2</sub><sup>+</sup>. Note that the overall electron stoichiometry of the mechanism in Eqs. A1-A4 is equal to ¼ electrons since one unreacted V<sup>IV</sup>O(acac)<sub>2</sub> is consumed by the ligand exchange in Eq. A2 and an additional two equivalents of  $V^{IV}O(acac)_2$  are consumed in Eq. A4 (see Eq. A5).

 $V^{IV}O(acac)_2 + \frac{1}{4} H_2O \rightarrow \frac{1}{4} V^{IV}O(OH)(acac) + \frac{1}{2} V^VO(acac)_2^+ + \frac{1}{4} V^{IV}O(OH)(acac)_2^+ + \frac{1}{4$  $V^{III}(acac)_3 + \frac{1}{4}OH^- + \frac{1}{4}e^-$  (A.5).

It is also noteworthy that the proposed mechanism is expected to generate an additional two equivalents of VVO(acac) that can further react extremely fast with free ligand and generate additional V<sup>III</sup>(acac)<sub>3</sub> near the generator electrode. This global stoichiometry would even be more complex if V<sup>IV</sup>O(OH) (acac) is oxidizable at the oxidation wave of  $V^{IV}O(acac)_2$ :

 $V^{IV}O(OH)(acac) \leftrightarrow V^{V}O(OH)(acac)^{+} + e^{-}$  (A.6). as suggested by the absence of a reduction wave that could be ascribed to this species in the CV of the V<sup>IV</sup>O(acac)<sub>2</sub>/V<sup>III</sup>(acac)<sub>3</sub> redox system. This may look unlikely at first glance, however, one expects the resulting  $V^{V}O(OH)(acac)^{+}$  species to react much faster in the presence of adventitious water with the parent VIVO(acac)<sub>2</sub> species than  $V^{V}O(acac)_{2}^{+}$ :

 $V^{V}O(OH)$  (acac)<sup>+</sup> + 2  $V^{IV}O(acac)_2$  +  $H_2O \rightarrow V^{III}(acac)_3$  + 2  $V^{V}O_{2}^{+} + 3OH^{-}$  (A.7).

Eq. (A6) may thus displace the oxidation wave of V<sup>IV</sup>O(acac)<sub>2</sub> much before its standard potential [43] so that it may occur before that of V<sup>IV</sup>O(acac)<sub>2</sub>. The result is that a complicated sequence of electrochemical and chemical events may take place at the potential of the VIVO(acac)2 oxidation wave leading to a variety of unstable species and further convoluting the number of electrons passed per vanadyl unit. In other words, depending on the extent of the conversion in Eqs. A6 and A7, the electron stoichiometry of V<sup>IV</sup>O(acac)<sub>2</sub> is expected to be at least ¼ e<sup>-</sup> and possibly ranging to larger values. If one were relying on RDE measurements of

V<sup>IV</sup>O(acac)<sub>2</sub> oxidation, using the limiting plateau current in RDE would require a foreknowledge of the value, n, the apparent number of electrons exchanged per V<sup>IV</sup>O(acac)<sub>2</sub> that would prevail for the RDE rotation rate in order to determine the diffusion coefficient of the products. Similarly, current feedback measurements in SECM are highly dependent on the ability of VIVO(acac)2 to be quantitatively regenerated by oxidation of V<sup>III</sup>(acac)<sub>3</sub> at the collector which cannot be guaranteed within the short time scales of SECM experiments. Conversely, ETOF measurements rely exclusively on diffusional time durations of the V<sup>III</sup>(acac)<sub>3</sub> species and not at all on current intensities.

#### References

- [1] C.D. Johnson, D.W. Paul, Sens, Actuators, B 105 (2005) 322.
- [2] C. Amatore, J.M. Saveant, J. Electroanal. Chem. Interfacial Electrochem. 126
- O. Liu, A.E.S. Sleightholme, A.A. Shinkle, Y. Li, L.T. Thompson, Electrochem. Commun 11 (2009) 2312
- R.D. Martin, P.R. Unwin, Anal. Chem. 70 (1998) 276.
- R.D. Martin, P.R. Unwin, J. Chem. Soc., Faraday Trans. 94 (1998) 753.
- R.D. Martin, P.R. Unwin, J. Electroanal. Chem. 439 (1997) 123.
- C.G. Zoski, J.C. Aguilar, A.J. Bard, Anal. Chem. 75 (2003) 2959.
- C.G. Zoski, B. Liu, A.J. Bard, Anal. Chem. 76 (2004) 3646.
- C.G. Zoski, C.R. Luman, J.L. Fernandez, A.J. Bard, Anal. Chem. 79 (2007) 4957.
- [10] G. Che, Z. Li, H. Zhang, C.R. Cabrera, J. Electroanal. Chem. 453 (1998) 9.
- [11] A.M. Lehaf, M.D. Moussallem, J.B. Schlenoff, Langmuir 27 (2011) 4756.
- [12] T.H. Silva, S.V.P. Barreira, C. Moura, F. Silva, Port. Electrochim. Acta 21 (2003)
- [13] R.A. Ghostine, J.B. Schlenoff, Langmuir 27 (2011) 8241.
- H. Dong, X. Cao, C.M. Li, ACS Appl. Mater. Interfaces 1 (2009) 1599.
- [15] M. Strawski, M. Szklarczyk, J. Electroanal. Chem. 624 (2008) 39.
- A.I. Bhatt, R.A.W. Dryfe, J. Electroanal. Chem. 584 (2005) 131.
- A.I. Gopalan, K.-P. Lee, K.M. Manesh, P. Santhosh, J.H. Kim, J. Mol. Catal. Chem. 256 (2006) 335.
- C. Amatore, M. Azzabi, P. Calas, A. Jutand, C. Lefrou, Y. Rollin, J. Electroanal. Chem. Interfacial Electrochem. 288 (1990) 45.
- C. Amatore, G. Capobianco, G. Farnia, G. Sandona, J.M. Saveant, M.G. Severin, E. Vianello, J. Am. Chem. Soc. 107 (1985) 1815.
- B. Fosset, C. Amatore, J. Bartelt, R.M. Wightman, Anal. Chem. 63 (1991) 1403.
- J. Ghilane, C. Lagrost, P. Hapiot, Anal. Chem. 79 (2007) 7383.
- [22] B.J. Feldman, S.W. Feldberg, R.W. Murray, J. Phys. Chem. 91 (1987) 6558.
- C. Amatore, C. Sella, L. Thouin, J. Electroanal. Chem. 593 (2006) 194.
- S. Licht, V. Cammarata, M.S. Wrighton, J. Phys. Chem. 94 (1990) 6133.
- [25] D. Ky, C.K. Liu, C. Marumoto, L. Castaneda, K. Slowinska, J. Contr. Release 112
- K. Slowinska, M.J. Johnson, M. Wittek, G. Moller, M. Majda, Proc. Electrochem. Soc. 18 (2001) 130, 2001.
- [27] K. Slowinska, M. Majda, J. Solid State Electrochem. 8 (2004) 763.
- [28] H.B. Tatistcheff, I. Fritsch-Faules, M.S. Wrighton, J. Phys. Chem. 97 (1993)
- J. Moldenhauer, M. Meier, D.W. Paul, J. Electrochem. Soc. 163 (2016) H672.
- [30] N. Baltes, L. Thouin, C. Amatore, J. Heinze, Angew. Chem. Int. Ed. 43 (2004)
- C. Amatore, N. Da Mota, C. Sella, L. Thouin, Anal. Chem. 80 (2008) 4976.
- S.E. Fosdick, K.N. Knust, K. Scida, R.M. Crooks, Angew. Chem. Int. Ed. 52 (2013)
- [33] A. Oleinick, J. Yan, B. Mao, I. Svir, C. Amatore, ChemElectroChem 3 (2016) 487.
- C. Amatore, Y. Bouret, E. Maisonhaute, J.I. Goldsmith, H.D. Abruna, Chem-PhysChem 2 (2001) 130.
- [35] M.A. Nawi, T.L. Riechel, Inorg. Chem. 20 (1981) 1974.
- [36] A. Vincent, Educ. Chem. 34 (1997) 165.
- [37] N.G. Tsierkezos, J. Solut, Chem. 36 (2007) 289.
- [38] D.P. Valencia, F.J. Gonzalez, J. Electroanal. Chem. 681 (2012) 121.
- S.I. Konopka, B. McDuffie, Anal. Chem. 42 (1970) 1741.
- [40] M.A. Nawi, T.L. Riechel, Inorg. Chem. 21 (1982) 2268.
- J.S. Shamie, C. Liu, L.L. Shaw, V.L. Sprenkle, ChemSusChem 10 (2017) 533.
- A.A. Shinkle, A.E.S. Sleightholme, L.D. Griffith, L.T. Thompson, C.W. Monroe, Power Sources 206 (2012) 490.
- [43] L. Nadjo, J.M. Saveant, J. Electroanal. Chem. Interfacial Electrochem. 48 (1973) 113